CD137 Agonist Induces Gastric Cancer Cell Apoptosis by Enhancing The Functions of CD8+ T Cells via NF-κB Signaling

Ben-Shun Hu
Nanjing Medical University
Tian Tang
Nanjing Medical University
Tie-Long Wu
Jiangnan University
Ying-Yue Sheng
Jiangnan University
Yu-Zheng Xue (xueyz001@163.com)
Jiangnan University

Research

Keywords: CD137, gastric cancer, CD8+ T cells, immune microenvironment.

Posted Date: July 10th, 2020

DOI: https://doi.org/10.21203/rs.3.rs-40870/v1

Version of Record: A version of this preprint was published at Cancer Cell International on October 20th, 2020. See the published version at https://doi.org/10.1186/s12935-020-01605-0.

Abstract

Background: CD137 is identified as a target for tumor immunotherapy. However, the role of CD137 in gastric cancer (GC), especially in inducing GC cell apoptosis has not been studied yet.

Methods: $Foxp3^+$ and $CD8^+$ T cells in GCs were investigated by immunohistochemistry (IHC). CD137 expression in GCs was detected by flow cytometry, IHC and immunofluorescence (IF). Peripheral blood mononuclear cells (PBMCs) and $CD8^+$ T cells isolated from peripheral blood were stimulated with a CD137 agonist in vitro. $CD8^+$ T cells proliferation and p65 expression were explored by flow cytometry. p65 nuclear translocation was analyzed by IF. IL-10, TGF-β, IFN-γ, Perforin and Granzyme B were detected by real-time quantitative PCR (real-time PCR). PBMCs and primary GC cells were cocultured and stimulated with the CD137 agonist in vitro. Apoptosis of the primary GC cells was detected by flow cytometry.

Results: Our data demonstrated that GC tumors show characteristics of an immunosuppressive microenvironment. CD137 was predominantly expressed in $CD8^+$ T cells in GCs and had a positive correlation with tumor cell differentiation. CD137 agonist promoted $CD8^+$ T cells proliferation and increased the secretion of IFN-γ, Perforin and Granzyme B, which induced primary GC cell apoptosis. Mechanistically, this study found that CD137 agonist could induce NF-κB nuclear translocation in $CD8^+$ T cells.

Conclusion: Our results demonstrate that CD137 agonist can induce primary GC cell apoptosis by enhancing $CD8^+$ T cells via activating NF-κB signaling.

Background

Gastric cancer (GC) is a common malignant tumor. Chemotherapy and molecular targeted therapy have achieved limited improvements in survival[1, 2]. Immunotherapy is a new method of tumor treatment in addition to surgery, chemotherapy and radiotherapy[3, 4]. It was reported initial T lymphocyte reaction was activated by vaccines, and an immune checkpoint activator can enhance the activity of T lymphocytes[5]. Adoptive immunotherapy was reported to achieve an antitumor effect via reinfusion of tumor-specific effector lymphocyte expanded in vitro[6]. Currently, immunosuppressive agents have shown a certain effect in the treatment of GC, while immune checkpoint agonists are less studied in GC.

CD137, also known as 4-1BB, is a member of the tumor necrosis factor (TNF) receptor family and is encoded by the TNF receptor superfamily member 9 (TNFRSF9) gene[7, 8]. Mouse CD137 is located at 75.5 cm on mouse chromosome 4 and exhibits approximately 60% homology with human CD137[9]. CD137 is mainly expressed in activated $CD8^+$ and $CD4^+$ T cells and in regulatory T cells (Tregs)[10, 11]. Accumulated animal experiments demonstrated that mice with a systemic deletion of CD137 genes showed the disordered immune homeostasis and lost the ability to fight against tumor immune memory. However, the role of CD137 in GC has not been investigated[12].

CD137 expression is upregulated on Antigen-presenting cells (APCs) as a result of activation of T cells initialed by B7-1, B7-2 and antigenic peptides, which promote the production and secretion of cytokines via activating NF-κB[13, 14]. It is now well established that CD137 induces the TNFR-related factors TRAF1 and TRAF2 to form a heterotrimer, which activates mitogen-activated protein kinase (MAPK), β-catenin and AKT signaling, and augments NF-κB nuclear translocation ultimately[15–17]. It's worth noting that the activation of NF-κB contributes to the survival of $CD8^+$ T lymphocytes by increasing the expression of the antiapoptotic genes Bcl-xL and bfl-l[11, 18]. However, whether CD137 mediated activation of NF-κB in $CD8^+$ T lymphocytes could induce GC cell apoptosis by enhancing the functions of $CD8^+$ T cells is unclear.

The most effective approach for CD137 agonist therapy is to stimulate the proliferation of $CD8^+$ T cells by increasing the expression of IFN-γ and several granzymes[19]. The CD137 costimulatory signal can be activated by a CD137 agonist or CD137L transfection, which can induce cell proliferation, cytokine expression and bactericidal activity and support T cell effector function[20]. Additionally, CD137 agonist can inhibit the differentiation of conventional effector cells into Tregs, negatively regulate the activity of Tregs, or maintain the expansion and inhibition of Tregs[21].

In this study, we demonstrate that GC tumors show the characteristic of an immunosuppressive microenvironment. CD137 agonist can induce primary GC cell apoptosis by enhancing $CD8^+$ T cells via activating NF-κB signaling.

Materials And Methods

Patients and specimens

For phenotypic assay, 23 fresh gastric cancerous, tumor margin and tumor-free gastric tissues (more than 1cm distance from the tumor), routinely paraffin-embedded for IHC and IF, were collected from 23 patients with GC who underwent surgery at our hospital between May 2019 and May 2020. At the same time, 23 fresh gastric cancerous tissues, isolated of tumor infiltrating lymphocytes (TILs) for flow cytometry, were collected. The clinical characteristics of the patients for phenotypic assay are listed in Table 1.

For functional assay, peripheral blood from 18 patients with GC was collected before surgery. 18 fresh gastric cancerous tissues were later collected during surgery. The clinical characteristics of the patients for functional assay are listed in Table 2.

All patients providing samples did not receive preoperative radiotherapy or chemotherapy and were confirmed to have GC by postoperative pathology. Informed consent for publication was obtained from all participants. This study has been conducted in accordance with ethical standards and according to the declaration of the national and international guidelines, and has been approved by the institutional review board of Jiangnan University.

Antibodies and reagents

RNAlater® was purchased from Ambion. TRIzol was purchased from Invitrogen. DEPC was purchased from Bio Basic Inc. The SYBR®PrimeScript® RT-PCR Kit was purchased from TaKaRa for two-step RT-PCR. PCR primers were designed by TaKaRa and synthesized by Yingjun Biotechnology Co., Ltd. An anti-CD137 rabbit mAb (#34549) used for IHC and IF was purchased Cell Signaling Technology (CST, USA). An IHC detection reagent (HRP, rabbit, #8114) was purchased from CST. An agnostic anti-CD137 mAb (#79097) was purchased from BPS Bioscience. An anti-Foxp3 rabbit mAb (#12653) used for IHC was purchased from CST. An anti-CD8 mouse antibody (#66868-1-Ig) for IHC and IF was purchased from Proteintech group. MojoSort™ Magnet, MojoSort™ Human CD8 Nanobeads and MojoSort™ Human CD8 Cell Isolation Kit were purchased from BioLegend. A NF-κB p65 rabbit mAb (#8242) for flow cytometry and IF was purchased from CST. An anti-Cytokeratin mouse mAb (#ab756) used for IHC was purchased from Abcam. A purified anti-human CD3 mAb (OKT3, #317326) for cell incubation, and anti-CD45-PerCP (#368506), anti-CD3-FITC (#300406), anti-CD8-APC (#301014) and anti-CD137-APC (#309809) antibodies for flow cytometry were purchased from BioLegend.

IHC assay

Fresh tissues or collected cells were fixed, dehydrated and paraffin embedded. Paraffin sections were dewaxed and rehydrated according to a routine protocol, and then antigen repair, neutralization of endogenous catalases, serum blocking, incubation with anti-CD137 rabbit mAb antibody (1:100, CST), anti-Foxp3 rabbit mAb antibody (1:100, CST) , anti-Cytokeratin mouse mAb antibody (1:100, Abcam) and anti-CD8 mouse antibody (1:100, Proteintech group) respectively at 4°C overnight, incubation with a secondary antibody, DAB color development, counterstaining, neutral gum sealing and observation were carried out step by step according to a standard immunohistochemical operation procedure. PBS was used as a negative control. The stained sections were scanned by Panoramic MIDI. Image J was used to count positive staining cells. The results were confirmed independently by two senior pathologist.

IF assay

For paraffin sections, paraffin sections of a specimen were dewaxed and sealed with 3% H_2O_2 for 10 min and then heat retrieved with 0.01 mmol/l citrate buffer (pH=6.0). After natural cooling, the sections were blocked with goat serum for 30 min, and then incubated with an anti-CD137 rabbit mAb (1:100, CST) and anti-CD8 mouse mAb (1:100, Proteintech group) overnight in a water tank at 4 ℃. After 1 h of rewarming, detected with anti-Rabbit IgG (H+L), F(ab')2 Fragment (Alexa Fluor® 594 Conjugate) and anti-Mouse IgG (H+L), F(ab')2 Fragment (Alexa Fluor® 488 Conjugate) (both 1:500, CST), the sections were incubated at 37 ℃ for 1 h, DAPI was added, and the sections were incubated in the dark for 5 min, sealed with 50% glycerol, and observed under a confocal microscope.

For cells IF, cells, after slide preparation, were fixed by 4% paraformaldehyde, and penetrated by 0.5% Triton X-100 at room temperature for 20min. the slides were blocked with goat serum for 30 min. and then incubated with an anti-NF-κB p65 rabbit mAb (1:100, CST) overnight in a water tank at 4 ℃. After 1

h of rewarming, detected with anti-Rabbit IgG (H+L), F(ab')2 Fragment (Alexa Fluor® 594 Conjugate) (1:500, CST) for 1h, DAPI was added, and the sections were incubated in the dark for 5 min, and observed under a fluorescence.

Isolation of TILs

The gastric cancerous tissue specimens were cut into 1-mm-diameter pieces with ophthalmic surgical scissors, and the appropriate amount of tissue digestive solution containing 2 mg/ml type IV collagenase and 0.25 mg/ml hyaluronidase was added, and then the samples were transferred to a 15-ml centrifuge tube. They were digested in a shaker at 37 ℃ for 30 min. The cell suspension obtained by digestion was filtered with a 70-μm sieve, and the filtered liquid was collected in a 50-ml centrifuge tube. Adding 10ml of 40% percoll, then adding 10 ml of 80% percoll below 40% percoll. and centrifuging at 2000 rpm for 20 min. TILs were absorbed between 40% percoll and 80% percoll.

Isolation of PBMCs and $CD8^+$ T cells

After transferring 20 ml of blood obtained from patients with GC into 50-ml centrifuge tubes, adding 10 ml of PBS to dilute the blood, mixing gently, adding 10 ml of Ficoll lymphocyte separation solution to the bottom of 50-ml centrifuge tubes, and centrifuging at 2000 rpm for 20 min, lymphocytes were absorbed and washed twice with PBS for 5 min each time. After PBMCs was isolated, washed with MojoSort™ buffer once. The following experimental procedure for CD8 isolation protocol was according to MojoSort™ Human CD8 T Cell Isolation Kit given by BioLegend.

Isolation of primary GC cells

Live gastric cancerous specimens were immersed in sterilized PBS containing 200 U/ml penicillin and streptomycin for 10 min and then washed with sterilized PBS containing 1000 U/ml penicillin and streptomycin 5 times. The specimens were immersed in sterilized PBS containing 200 U/ml penicillin and streptomycin for 10 min to remove the blood stain and bacteria on the surface of the specimens. The tissue specimens were cut into 1-mm-diameter pieces with ophthalmic surgical scissors, and the appropriate amount of tissue digestive solution containing 2 mg/ml type IV collagenase and 0.25 mg/ml hyaluronidase was added, and then the samples were transferred to a 15-ml centrifuge tube. They were digested in a shaker at 37 ℃ for 30 min. The cell suspension obtained by digestion was filtered with a 70-μm sieve, and the filtered liquid was collected in a 50-ml centrifuge tube, adding 10 ml of Ficoll lymphocyte separation solution to the bottom of 50-ml centrifuge tubes, and centrifuging at 2000 rpm for 20 min for removing lymphocytes. Cells at the bottom of 50-ml centrifuge tubes were collected, added with erythrocyte lysate for 10 min to remove red cells. Then cells were washed with sterile PBS containing 1000 U/ml penicillin and streptomycin 5 times.

Primary GC cells and $CD8^+$ T cells stained with CFSE

Primary GC cells and $CD8^+$ T cells were collected and washed with PBS 3 times for 5 min each time. The primary GC cells were treated with 1 ml of 5 μM CFSE, cultured in a 37 ℃ CO_2 incubator for 15 min, added with 1 ml of fetal bovine serum to stop staining for 1 minute, and then washed twice with PBS.

Cell culture

CFSE-labeled $CD8^+$T cells, PBMCs or/and CFSE-labeled primary GC cells isolated from GC patients were added to 96-well plates (coated with a purified anti-human CD3 antibody at 5 μg/ml overnight to upregulate CD137 expression) and cultured in DMEM with 10% FBS.

Flow cytometry

For CD137 detection, the PBMCs or TILs of GC patients were placed in flow tubes, and 5 μL each of anti-CD45-PerCP antibody, anti-CD3-FITC antibody and anti-CD137-APC antibody was added. The cells were incubated in the dark for 10 min and washed with PBS once. Then, 200 μL of PBS was added for flow cytometry detection.

For examination of $CD8^+$ T cells proliferation, $CD8^+$ T cells of GC patients were placed in flow tubes. After washing with PBS once, 200 μL of PBS was added for flow cytometry detection.

For NF-κb detection, $CD8^+$ T cells from GC patients treated with 10 μg/ml agonistic anti-CD137 mAb for 72h were placed in flow tubes. After washing with PBS once, Fixation/Permeabilization Solution (BD Cytofix/Cytoperm^{TM}) were added at room temperature for 30 min. After washing with PBS once, A NF-κB p65 rabbit mAb (1:1000, CST) was added. The cells were incubated in the dark for 1 h and washed with PBS once. Adding 5 μl anti-rabbit IgG (H+L), F(ab')2 Fragment (Alexa Fluor® 594 Conjugate) (1:500, CST) and incubating the cells in the dark for 30 min. After washing with PBS once, 200 μL of PBS was added for flow cytometry detection.

Primary GC cell apoptosis detected by flow cytometry

PBMCs (1×10^5) and primary GC cells (2×10^4, CFSE stained) were mixed, placed in anti-human CD3 antibody coated 96-well plates containing 200 μl of 10% FBS DMEM, and then treated with 10 μg/ml agonistic anti-CD137 mAb. Apoptosis in the GC cells was detected by flow cytometry after 72 h.

RNA extraction and reverse transcription

The TRIzol method was used to extract total RNA from cultured cells for RNA quantitative analysis and RNA electrophoresis. The conditions of the reverse transcriptase reaction were 42 ℃ for 15 min and inactivation of the reverse transcriptase at 95 ℃ for 2 min. After the above reaction, the reverse transcriptase solution was added to a real-time PCR system. The reaction solution was stored at -20 ℃ until use. The DNA concentration was estimated from the A260/A280 value detected with a spectrophotometer.

Based on the cDNA sequences of IL-10, TGF-β, IFN-γ, Perforin, Granzyme B and the housekeeping gene β-actin, real-time fluorescent quantitative PCR oligonucleotide primers were designed with Primer Premier 5 software. The sequences were specific by BLAST. The following primer sequences were designed and synthesized by TaKaRa. Primers for specific genes in this study were listed in **Table 3**. For real-time PCR amplification, sample analysis was performed as follows: each group contained three duplicate detection tubes, each sample was evenly mixed, centrifuged, tested by computer, amplified by fluorescence quantitative PCR, and produced an amplification curve. The reaction process was as follows: predenaturation at 95 ℃ for 5 min, denaturation at 95 ℃ for 15 s, annealing at 58 ℃ for 15 s, elongation at 72 ℃ for 40 s (40 cycles). The corresponding software program of the real-time PCR instrument used recorded and analyzed the detection data and output the results. According to the $2^{-\triangle\triangle CT}$ method, the relative expression of each target gene was calculated, and the amplification of the target gene was compared between each experimental group and the control group.

Statistical analysis

Statistical analysis was performed by GraphPad Prism 6 software. All data are shown as mean ± standard error of the mean (SEM). An unpaired two-tailed Student t test was employed for comparison between two groups. One-way ANOVA was employed for multiple comparisons. Error Significant p-values are labeled with one or more '*', denoting *p < .05, **p < .01, ***p < .001 and ****p < .0001. A threshold of P < 0.05 was defined as statistically significant.

Results

Poor infiltration of $CD8^+$ T cells but accumulation of Tregs in GCs

To compare the composition of $CD8^+$ and Treg cells in the tumor tissues, tumor-free tissues and tumor margin tissues of GC patients, we analyzed the proportions of $CD8^+$ T cells and $Foxp3^+$ Tregs by IHC. $Foxp3^+$ Tregs were accumulated in the tumor (**Fig. 1 A and B**), but the majority of $CD8^+$ T cells was sequestered at the tumor margin and tumor-free tissues (**Fig. 1 C and D**). These data suggested that $CD8^+$ T cells were excluded from the tumors and $Foxp3^+$ Tregs infiltrated into the tumors of GC patients.

CD137 was highly expressed in differentiated tumor and mainly expressed in $CD8^+$ T cells in GCs

To analyze CD137 expression in GCs, we first examine CD137 exression in TILs of GC patients. Interestingly, CD137 expression was highly expressed in differentiated tumor (**Fig. 2 A and B**). This result was later confirmed by IHC and IF (**Fig. 2 C and D**). Furthermore, IF showed that CD137 was mainly expressed in $CD8^+$ TILs (**Fig. 3 A**). Thus, we focused on CD137 functions on $CD8^+$ T cells.

An agonistic anti-CD137 mAb can enhance $CD8^+$ T cells proliferation and increase its secretion of IFN-γ, Perforin and Granzyme B but has little effect on Tregs in GC

To determine the role of CD137 in the immune microenvironment of GC, $CD8^+$ T cells were isolated from peripheral blood in GC patients (**Fig. 3 B, C, D and E**) and stimulated with a CD137 agonist. CFSE-labeled $CD8^+$ T cells proliferation were observed in the presence of an agonistic anti-CD137 mAb (**Fig. 3 F and G**). Next, we examined the overall effect of the CD137 agonist in GC patients. PBMCs were isolated from peripheral blood in GC patients. For Tregs, secretion of IL-10 and TGF-β, play a role in maintaining immune tolerance, IL-10 and TGF-β were detected by real-time PCR. Our results showed that IL-10 and TGF-β was almost unchanged in the presence of a CD137 agonist (**Fig. 4 A and B**). Interestingly, the CD137 agonist could increase the production of IFN-γ, Perforin and Granzyme B (**Fig. 4 C, D and E**), secretion from $CD8^+$ T cells, in the PBMCs from GC patients. Together, these results demonstrated that the function of $CD8^+$ T cells was enhanced in the presence of a CD137 agonist.

NF-κB expression and nuclear translocation were increased in $CD8^+$ T cells after CD137 agonist treatment

To examine the mechanism of CD137 in $CD8^+$ T cells, NF-κB subunit p65 expression and nuclear translocation were detected. p65 expression was significantly increased in $CD8^+$ T cells in the presence of a CD137 agonist (**Fig. 5 A and B**). In addition, a CD137 agonist could induce p65 nuclear translocation in $CD8^+$ T cells (**Fig. 5 C**).

A CD137 agonist can induce apoptosis in primary GC cells

Finally, we investigated the effect of the CD137 agonist on primary GC cells. HE staining combined with IHC□Cytokeratin antibody was helpfully used to confirm tumors□were used to examine the purity of primary GC cells after isolation (**Fig. 6 A, B and C**). To further study the function of a CD137 agonist in the immune microenvironment of GC, we cocultured PBMCs and CFSE-labeled primary GC cells at a ratio of 5:1 in vitro in the presence of 10 μg/ml agonistic anti-CD137 mAb. Flow cytometry was used to detect primary GC cell apoptosis after 72 h. Compared with control treatment, the CD137 agonist could induce apoptosis in the primary GC cells (**Fig. 6 D and E**).

Discussion

Morbidity and mortality of GC are high among all malignant tumors, and the clinical therapeutic effect of monoclonal antibodies against a single target in GC is limited[6, 22, 23]. In order to improve the curative effect and reduce drug resistance, it's urgent to find specific monoclonal antibody in the treatment for GC[24, 25]. Immune escape is considered as an important process of tumor development. We also found the immunosuppressive microenvironment that $CD8^+$ T cells were excluded from the tumors, while $Foxp3^+$ Tregs infiltrated into the tumors of GC patients. At present, CD137/CD137L targeted therapy has been shown to be effective against melanoma, leukemia and other tumors[26]. In this study, the effect of CD137 on the immune microenvironment of GC was studied to provide new ideas for the treatment of GC.

It was demonstrated that CD137/CD137L activation signaling promote the activation and proliferation of tumor-specific T cells, increase the secretion of cytokines, and protect T cells from activation-induced cell

death[27, 28]. Tumors established by subcutaneous inoculation of Agl04A sarcoma or 10815 mast cells into mice could be eliminated by intraperitoneal administration of an anti-CD137 monoclonal antibody on the third or seventh day after inoculation, respectively[24]. Enhanced immune response was mainly mediated by $CD8^+$ T cells activated by the anti-CD137 monoclonal antibody and also accompanied by a significant enhancement in tumor-specific cytotoxic T lymphocytes (CTLs)activity[29]. For $CD4^+$ T cells, CD137/CD137L signal transduction can induce cell expansion but cannot prolong cell survival[30]. CD137 is mainly expressed on the surface of activated T cells, and our study found that CD137 was predominantly expressed on the surface of $CD8^+$ T cells in the GC immune microenvironment and may positively correlated with tumor differentiation.

CD137 has a more restricted number of TRAF family members involved in its regulation, since only TRAF1, TRAF2, and TRAF3 interact with and control CD137 activity[31]. It was reported that CD137 signalosome getting recruited by K63-polyubiquitinated TRAF2 is a kinase complex composed by the transforming growth factor beta-activated kinase (TAK)-1, which will phosphorylate the inhibitor of nuclear factor κ-B kinase (IKK)-β leading to the activation of canonical NF-κB[32]. Our results showed that CD137 agonist could enhance $CD8^+$ T cells proliferation. Additionally, CD137 agonist could increase p65 expression and induce nuclear p65 nuclear translocation in $CD8^+$ T cells. IL-10 and TGF-β, secretion from Tregs, play a critical role in maintaining immune tolerance. Thus, we consider the effect of CD137 agonist on Tregs. Our data suggest that the CD137 agonist could increase the secretion of IFN-γ, Perforin and Granzyme B in the $CD8^+$ T cells and had little effect on Tregs in the PBMCs from GC patients. In this study, CD137 agonist could significantly induce apoptosis in the primary GC cells upon PBMCs and primary GC cells were cocultured, which imply CD137 agonist as an adaptor in the immune microenvironment of GC.

Conclusions

$CD8^+$ T cells were excluded from the tumors and $Foxp3^+$ Tregs infiltrated into the tumors in GC patients. CD137 is mainly expressed on CD8-positive T cells in the GC immune microenvironment. A CD137 agonist can enhance $CD8^+$ T cells proliferation via NF-κB signaling and increase the secretion of IFN-γ, Perforin and Granzyme B, but has little effect on Tregs in GC. Furthermore, CD137 agonist can induce apoptosis in primary GC cells. This study is expected to provide new ideas for the treatment of GC and has potential translational value.

Abbreviations

GC: gastric cancer; IHC: immunohistochemistry; IF: immunofluorescence; PBMCs: peripheral blood mononuclear cells; Real-time PCR: real-time quantitative PCR; TILs: tumor infiltrating lymphocytes; TNF: tumor necrosis factor; TNFRSF9: TNF receptor superfamily member 9; Tregs: regulatory T cells; APCs: antigen-presenting cells; DCs: dendritic cells; JNK: c-Jun N-terminal kinase; ERK: extracellular signal regulated kinase; CTLs: tumor-specific cytotoxic T lymphocytes.

Declarations

Acknowledgments

Not applicable.

Author Contributions

Ben-Shun Hu, and Yu-Zheng Xue conceived the study and designed the experiments; Ben-Shun Hu performed in vitro experiments; Tian Tang performed immunohistochemical staining and immunofluorescence; Yin-Yue Sheng and Tie-Long Wu organized the clinical samples and analyzed the data; Ben-Shun Hu wrote the manuscript; Yu-Zheng Xue modified the manuscript. All authors read and approved the final manuscript.

Funding

This study was supported by the Postgraduate Research & Practice Innovation Program of Jiangsu Province (KYCX19_1123), Wuxi City Health and Health Committee Youth Project (Q201919), Top Talents Project of the "Six-one Project" for High-level Health Talents in Jiangsu Province (LGY2018016), Application and Translation of Key Techniques on Gastrointestinal Lubricant (ZM008), and Key Talents Project of "Strengthening Health through Science and Education" of Wuxi Health and Family Planning Commission (ZDRC039). This study is also a Wuxi Science and Technology Development Medical and Health Guidance Plan.

Availability of data and material

Data and materials are available for sharing if needed.

Ethics approval and consent to participate

This study has been conducted in accordance with ethical standards and according to the Declaration of the national and international guidelines, and has been approved by the authors' institutional review board. The study protocol was approved by the Medical Ethics Committee of Jiangnan University.

Consent for publication

Informed consent for publication was obtained from all participants.

Competing interests

The authors declare that they have no competing interests.

References

1. Arai H, Nakajima TE: Recent Developments of Systemic Chemotherapy for Gastric Cancer. Cancers (Basel) 2020, 12(5).
2. Yao S, Yan W: Overexpression of Mst1 reduces gastric cancer cell viability by repressing the AMPK-Sirt3 pathway and activating mitochondrial fission. Onco Targets Ther 2018, 11:8465-8479.
3. Abdul-Latif M, Townsend K, Dearman C, Shiu KK, Khan K: Immunotherapy in gastrointestinal cancer: The current scenario and future perspectives. Cancer Treat Rev 2020, 88:102030.
4. Tan S, Xia L, Yi P, Han Y, Tang L, Pan Q, Tian Y, Rao S, Oyang L, Liang J et al: Exosomal miRNAs in tumor microenvironment. J Exp Clin Cancer Res 2020, 39(1):67.
5. Kono K, Nakajima S, Mimura K: Current status of immune checkpoint inhibitors for gastric cancer. Gastric Cancer 2020, 23(4):565-578.
6. Jones JO, Smyth EC: Gastroesophageal cancer: Navigating the immune and genetic terrain to improve clinical outcomes. Cancer Treat Rev 2020, 84:101950.
7. Wong HY, Schwarz H: CD137 / CD137 ligand signaling regulates the immune balance: A potential target for novel immunotherapy of autoimmune diseases. J Autoimmun 2020:102499.
8. Kang SW, Lee SC, Park SH, Kim J, Kim HH, Lee HW, Seo SK, Kwon BS, Cho HR, Kwon B: Anti-CD137 Suppresses Tumor Growth by Blocking Reverse Signaling by CD137 Ligand. Cancer Res 2017, 77(21):5989-6000.
9. Cannons JL, Chamberlain G, Howson J, Smink LJ, Todd JA, Peterson LB, Wicker LS, Watts TH: Genetic and functional association of the immune signaling molecule 4-1BB (CD137/TNFRSF9) with type 1 diabetes. J Autoimmun 2005, 25(1):13-20.
10. Lee SW, Vella AT, Kwon BS, Croft M: Enhanced CD4 T cell responsiveness in the absence of 4-1BB. J Immunol 2005, 174(11):6803-6808.
11. Sabbagh L, Pulle G, Liu Y, Tsitsikov EN, Watts TH: ERK-dependent Bim modulation downstream of the 4-1BB-TRAF1 signaling axis is a critical mediator of CD8 T cell survival in vivo. J Immunol 2008, 180(12):8093-8101.
12. Sabbagh L, Andreeva D, Laramee GD, Oussa NA, Lew D, Bisson N, Soumounou Y, Pawson T, Watts TH: Leukocyte-specific protein 1 links TNF receptor-associated factor 1 to survival signaling downstream of 4-1BB in T cells. J Leukoc Biol 2013, 93(5):713-721.
13. Kotanides H, Sattler RM, Lebron MB, Carpenito C, Shen J, Li J, Surguladze D, Haidar JN, Burns C, Shen L et al: Characterization of 7A5: A Human CD137 (4-1BB) Receptor Binding Monoclonal Antibody with Differential Agonist Properties That Promotes Antitumor Immunity. Mol Cancer Ther 2020, 19(4):988-998.
14. Shedlock DJ, Whitmire JK, Tan J, MacDonald AS, Ahmed R, Shen H: Role of CD4 T cell help and costimulation in CD8 T cell responses during Listeria monocytogenes infection. J Immunol 2003, 170(4):2053-2063.
15. Li G, Wu X, Zhang F, Li X, Sun B, Yu Y, Yin A, Deng L, Yin J, Wang X: Triple expression of B7-1, B7-2 and 4-1BBL enhanced antitumor immune response against mouse H22 hepatocellular carcinoma. J Cancer Res Clin Oncol 2011, 137(4):695-703.

16. Serghides L, Bukczynski J, Wen T, Wang C, Routy JP, Boulassel MR, Sekaly RP, Ostrowski M, Bernard NF, Watts TH: Evaluation of OX40 ligand as a costimulator of human antiviral memory CD8 T cell responses: comparison with B7.1 and 4-1BBL. J Immunol 2005, 175(10):6368-6377.
17. Arron JR, Pewzner-Jung Y, Walsh MC, Kobayashi T, Choi Y: Regulation of the subcellular localization of tumor necrosis factor receptor-associated factor (TRAF)2 by TRAF1 reveals mechanisms of TRAF2 signaling. J Exp Med 2002, 196(7):923-934.
18. McPherson AJ, Snell LM, Mak TW, Watts TH: Opposing roles for TRAF1 in the alternative versus classical NF-kappaB pathway in T cells. . J Biol Chem 2012, 287(27):23010-23019.
19. ZT F, TR N, DH H, RJ J, JJ E, MJ S, CM K, RY L, J Z, A G et al: A conserved intratumoral regulatory T cell signature identifies 4-1BB as a pan-cancer target. 2020, 130(3):1405-1416.
20. Hodge G, Hodge S, Reynolds PN, Holmes M: Targeting peripheral blood pro-inflammatory CD28null T cells and natural killer T-like cells by inhibiting CD137 expression: possible relevance to treatment of bronchiolitis obliterans syndrome. J Heart Lung Transplant 2013, 32(11):1081-1089.
21. Smith SE, Hoelzinger DB, Dominguez AL, Van Snick J, Lustgarten J: Signals through 4-1BB inhibit T regulatory cells by blocking IL-9 production enhancing antitumor responses. Cancer Immunol Immunother 2011, 60(12):1775-1787.
22. Reis-Dennis S: Review of Rethinking Health Care Ethics by Stephen Scher and Kasia Kozlowska : Palgrave Macmillan, available open access: https://link.springer.com/content/pdf/10.1007/978-981-13-0830-7.pdf. Monash Bioeth Rev 2020, 38(1):83-86.
23. Rocken C: Molecular classification of gastric cancer. Expert Rev Mol Diagn 2017, 17(3):293-301.
24. Ju SA, Lee SC, Kwon TH, Heo SK, Park SM, Paek HN, Suh JH, Cho HR, Kwon B, Kwon BS et al: Immunity to melanoma mediated by 4-1BB is associated with enhanced activity of tumour-infiltrating lymphocytes. Immunol Cell Biol 2005, 83(4):344-351.
25. Zhou G, Sprengers D, Mancham S, Erkens R, Boor PPC, van Beek AA, Doukas M, Noordam L, Campos Carrascosa L, de Ruiter V et al: Reduction of immunosuppressive tumor microenvironment in cholangiocarcinoma by ex vivo targeting immune checkpoint molecules. J Hepatol 2019, 71(4):753-762.
26. Sanchez-Paulete AR, Labiano S, Rodriguez-Ruiz ME, Azpilikueta A, Etxeberria I, Bolanos E, Lang V, Rodriguez M, Aznar MA, Jure-Kunkel M et al: Deciphering CD137 (4-1BB) signaling in T-cell costimulation for translation into successful cancer immunotherapy. Eur J Immunol 2016, 46(3):513-522.
27. MC SR, RA T, S B, HZ Q, AT H, AT V, Immunology AAJ, biology c: CD134/CD137 dual costimulation-elicited IFN-γ maximizes effector T-cell function but limits Treg expansion. 2013, 91(2):173-183.
28. Yang J, Park OJ, Lee YJ, Jung HM, Woo KM, Choi Y: The 4-1BB ligand and 4-1BB expressed on osteoclast precursors enhance RANKL-induced osteoclastogenesis via bi-directional signaling. Eur J Immunol 2008, 38(6):1598-1609.

29. J D, A P, C A, A A, MC O, A R, I M-F, A T, P B, A LB et al: Intratumoral injection of interferon-α and systemic delivery of agonist anti-CD137 monoclonal antibodies synergize for immunotherapy. 2011, 128(1):105-118.
30. Woroniecka KI, Rhodin KE, Dechant C, Cui X, Chongsathidkiet P, Wilkinson D, Waibl-Polania J, Sanchez-Perez L, Fecci PE: 4-1BB Agonism Averts TIL Exhaustion and Licenses PD-1 Blockade in Glioblastoma and Other Intracranial Cancers. Clin Cancer Res 2020, 26(6):1349-1358.
31. Zapata JM, Perez-Chacon G, Carr-Baena P, Martinez-Forero I, Azpilikueta A, Otano I, Melero I: CD137 (4-1BB) Signalosome: Complexity Is a Matter of TRAFs. Front Immunol 2018, 9:2618.
32. Li G, Boucher JC, Kotani H, Park K, Zhang Y, Shrestha B, Wang X, Guan L, Beatty N, Abate-Daga D et al: 4-1BB enhancement of CAR T function requires NF-kappaB and TRAFs. JCI Insight 2018, 3(18).

Tables

Table 1
Characteristics of patients for phenotypic data

	GC(23)
Sex(femal/male)	14/9
Age(years)**	58.2 ± 3.6
Histopathology	Highly differentiated GC = 6
	Poorly differentiated GC = 17
GC, gastric cancer. **Mean ± standard error of the mean.	

Table 2
Characteristics of patients for functional data

	GC(18)
Sex(femal/male)	7/11
Age(years)**	65.2 ± 3.1
Histopathology	Highly differentiated GC = 5
	Poorly differentiated GC = 13
GC, gastric cancer. **Mean ± standard error of the mean.	

Table 3
Real-time PCR primers description

Gene	Primer sequence	
	Forward (5’-3’)	Reverse (5’-3’)
β-actin	TGGCACCCAGCACAATGAA	CTAAGTCATAGTCCGCCTAGAAGCA
IL-10	GACTTTAAGGGTTACCTGGGTTG	TCACATGCGCCTTGATGTCTG
TGF-β	ACTTGCACCACCTTGGACTTC	GGTCATCACCGTTGGCTCA
IFN-γ	TCGGTAACTGACTTGAATGTCCA	TCGCTTCCCTGTTTTAGCTGC
Perforin	CGCCTACCTCAGGCTTATCTC	CCTCGACAGTCAGGCAGTC
Granzyme B	TGGGGGACCCAGAGATTAAAA	TTTCGTCCATAGGAGACAATGC

Figures

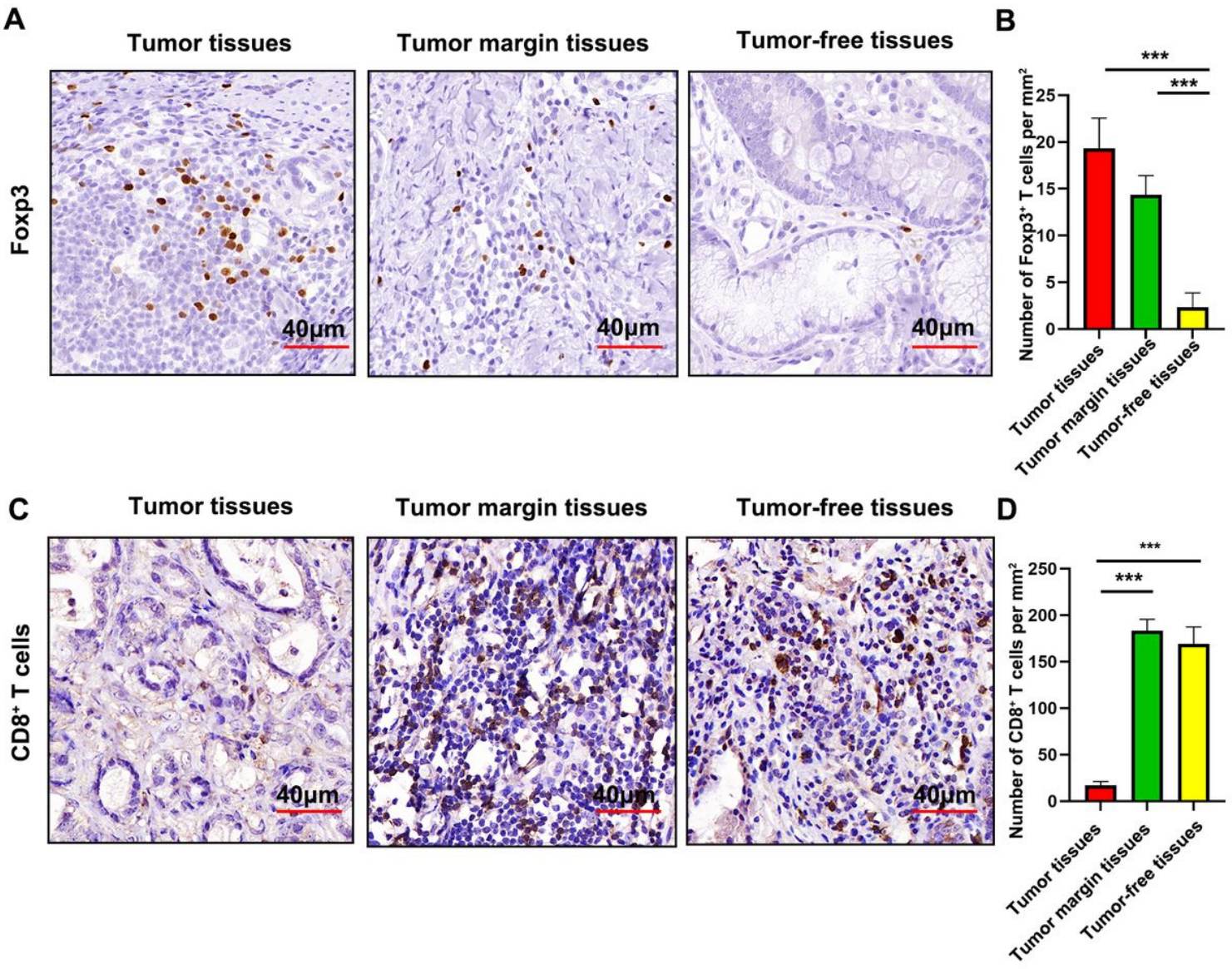

Figure 1

Poor infiltration of CD8+ T cells but accumulation of Tregs in gastric cancer. A, Foxp3 expression the GCs was detected by IHC. B, the cell densities of Foxp3 are depicted per square millimeter. Values are means with standard error of the mean. C, CD8 expression the GCs was detected by IHC. D, the cell densities of CD8 are depicted per square millimeter. Values are means with standard error of the mean.

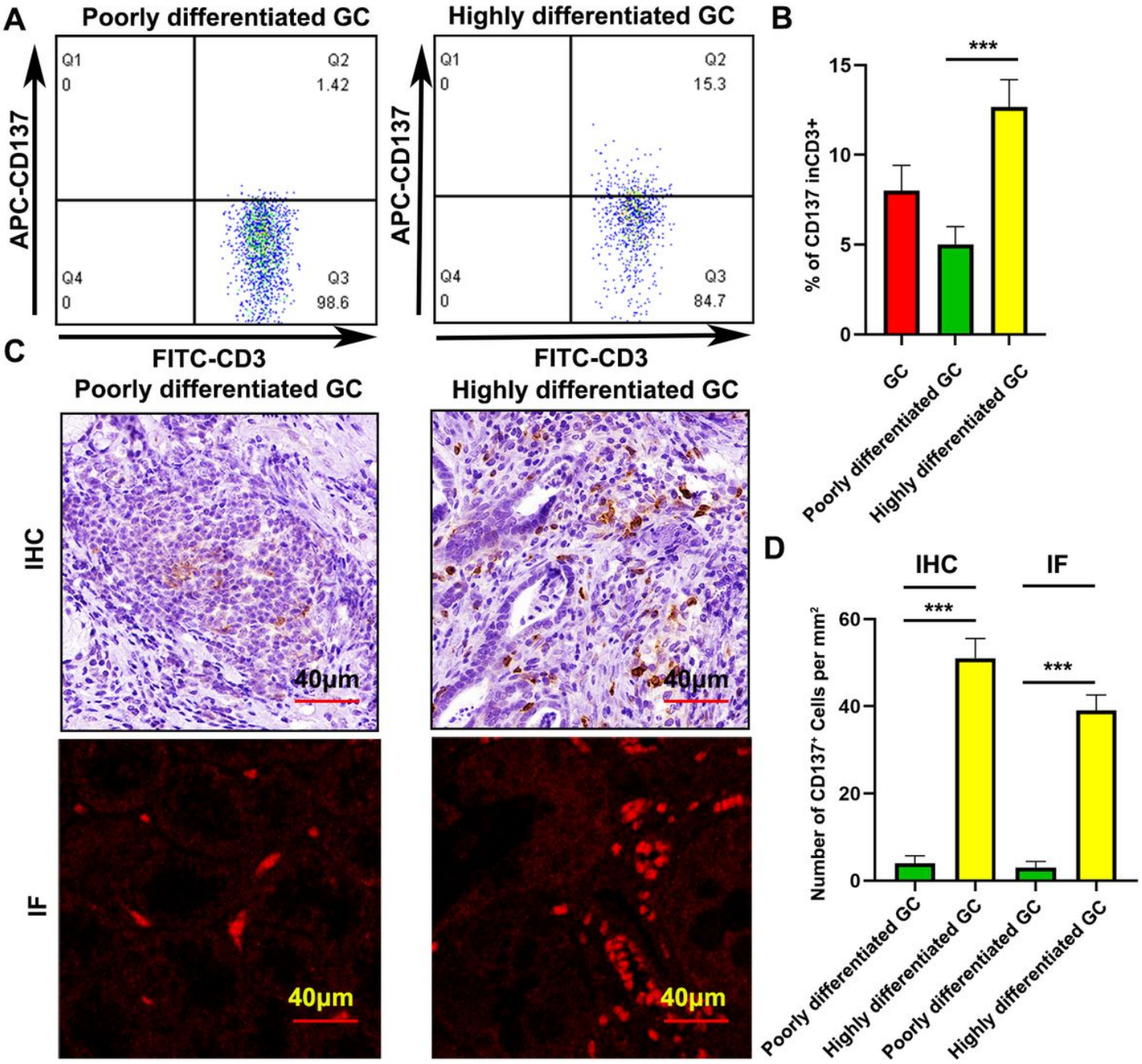

Figure 2

CD137 was highly expressed in TILs of GCs. A, CD137 expression in GCs was examined by flow cytometry. B, Statistical analysis of CD137 expression in different differentiation GCs. C, CD137 expression in GCs was measured by IHC and IF. D, Statistical analysis of CD137 expression in different differentiation GCs

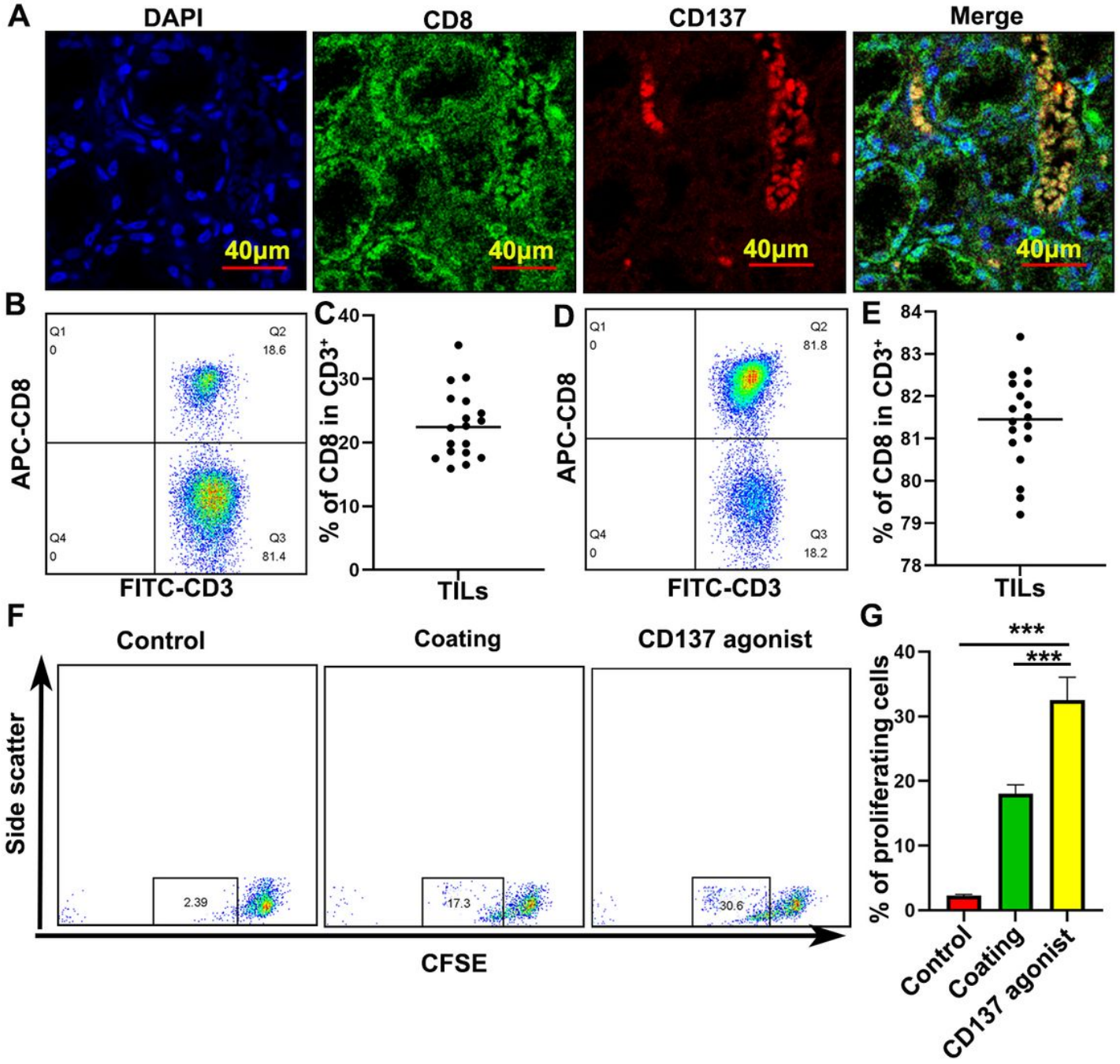

Figure 3

CD137 was mainly expressed in CD8+ T cells and CD 137 agonist could enhance CD8+ T cells proliferation. A, CD137 expression was examined by IF. B, the ratio of CD8 in CD3 before isolation. C, the ratio of CD8 in CD3 of individual patient before isolation are presented. D, the ratio of CD8 in CD3 after isolation. E, ratio of CD8 in CD3 of individual patient after isolation are presented. F, CD8+ T cells proliferation in response to CD 137 agonist. G, Values are means with standard error of the mean.

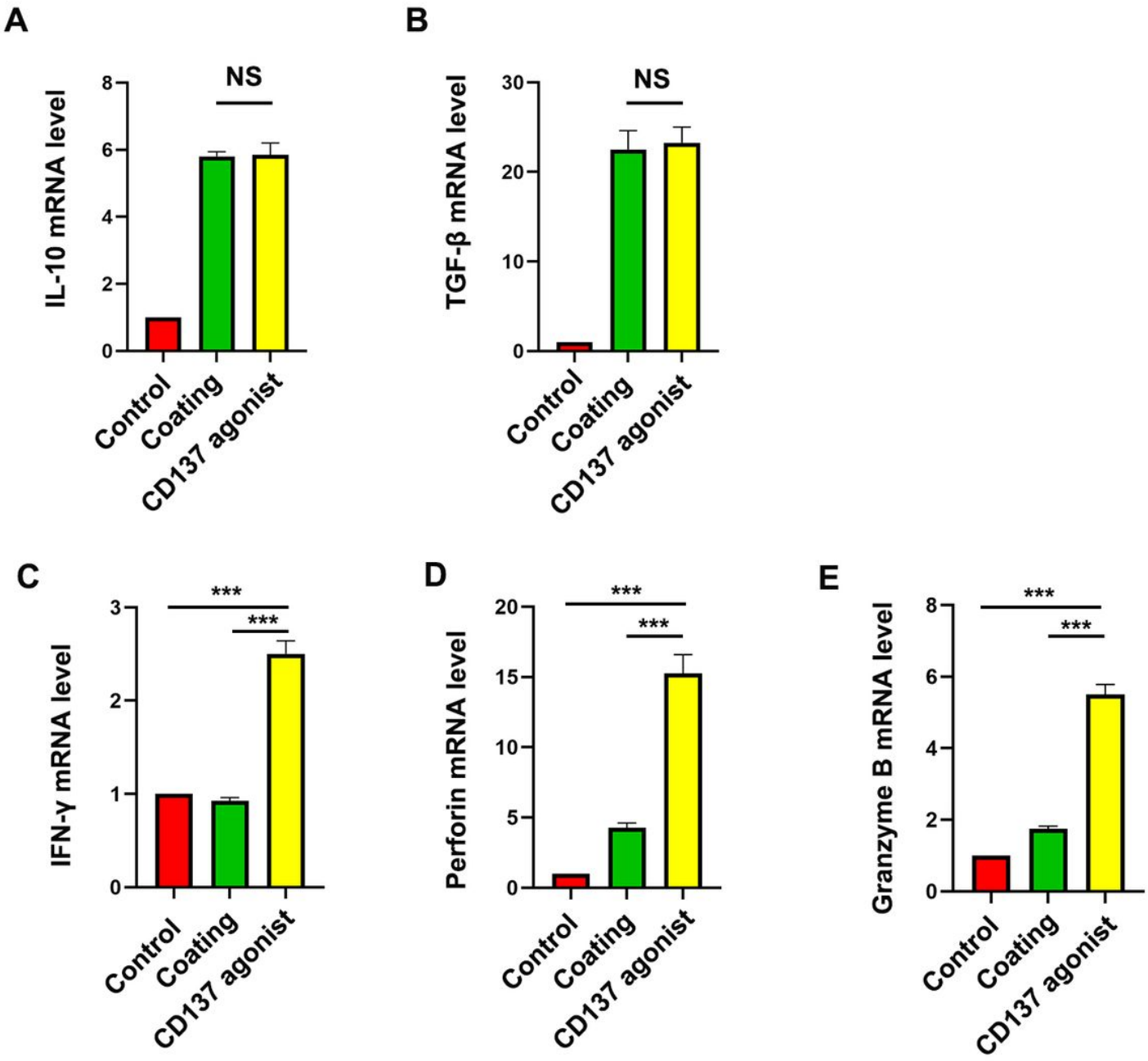

Figure 4

Functions of a CD137 agonist in the PBMCs of gastric cancer patients. A, IL-10 detected by real-time PCR. B, TGF-β detected by real-time PCR. C, IFN-γ detected by real-time PCR. D, Perforin detected by real-time PCR. E, Granzyme B detected by real-time PCR. NS=no significance.

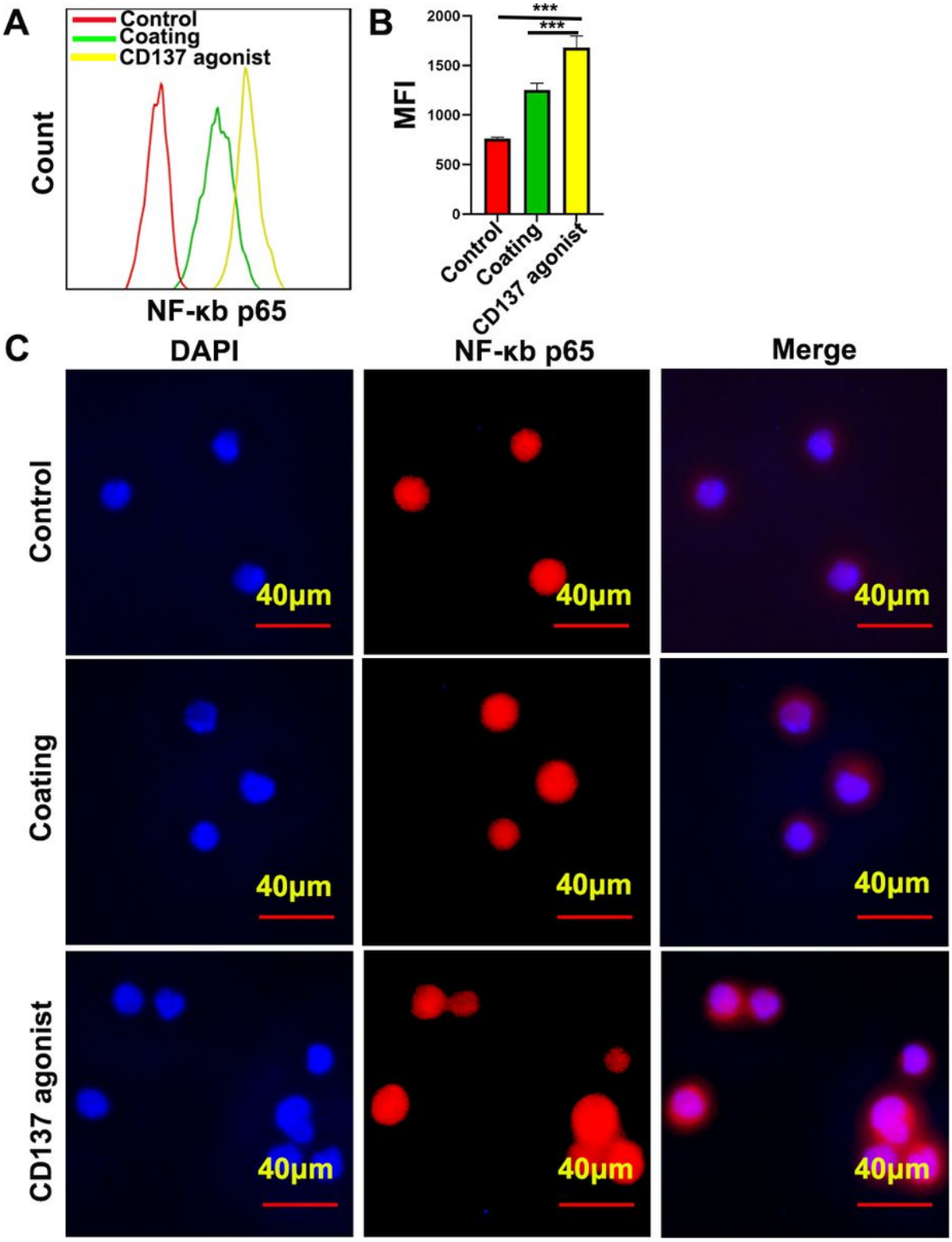

Figure 5

p65 expression and nuclear translocation were increased by targeting CD137. A, the effect of CD137 agonist one p65 expression was measured by flow cytometry. B, Values are means with standard error of the mean. C, the influence of CD137 agonist on p65 translocation was detected by IF.

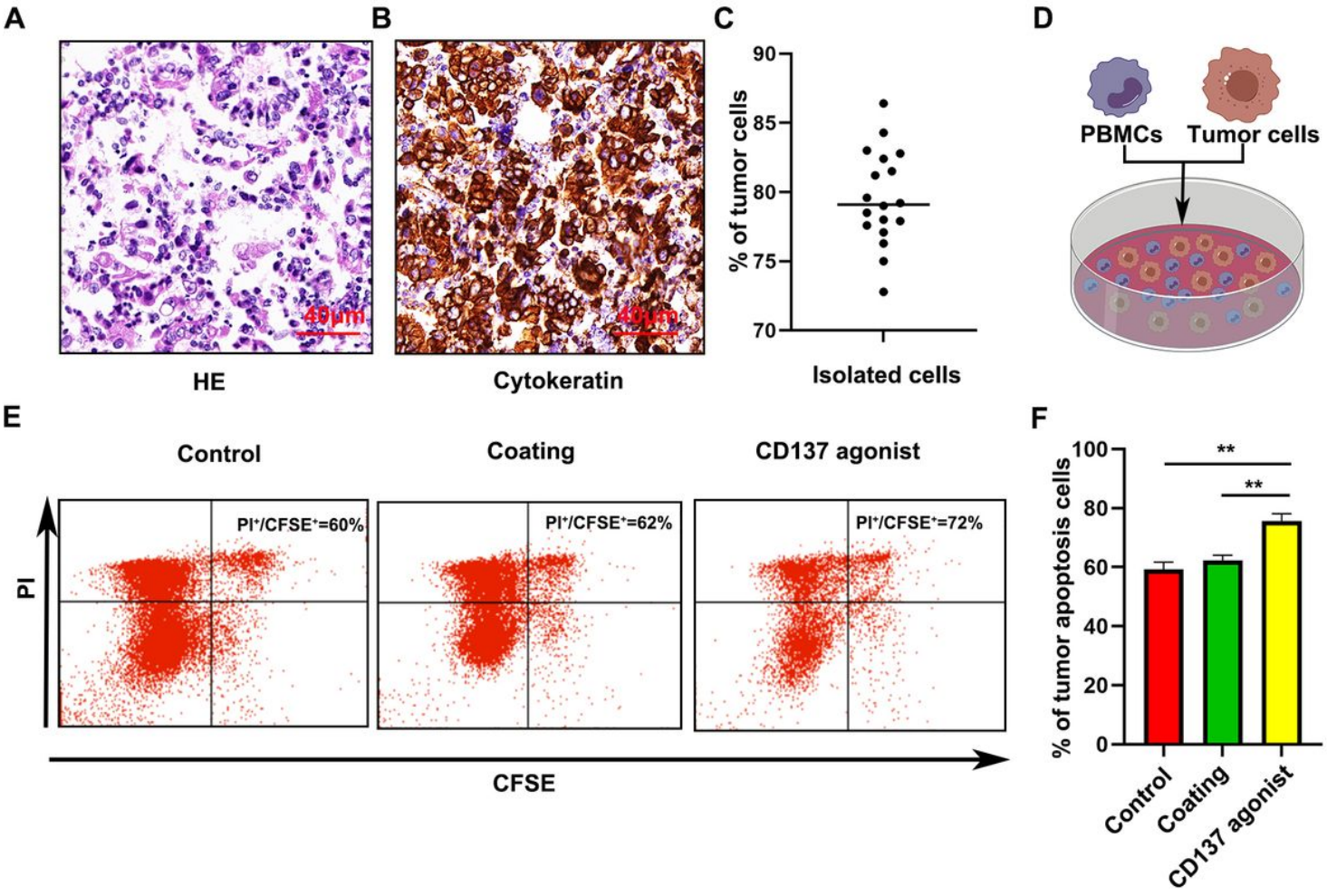

Figure 6

A CD137 agonist can significantly induce apoptosis in primary gastric cancer cells. A, the purity of isolation of tumor cells was detected by HE staining. B, IHC confirm the purity of isolation of tumor cells. C, the purity of individual patient after tumor isolation are presented. Values are means with standard error of the mean. D, Apoptosis of primary gastric cancer cells was detected by flow cytometry. E, Quantification of primary gastric cancer cell apoptosis. Values are means with standard error of the mean.

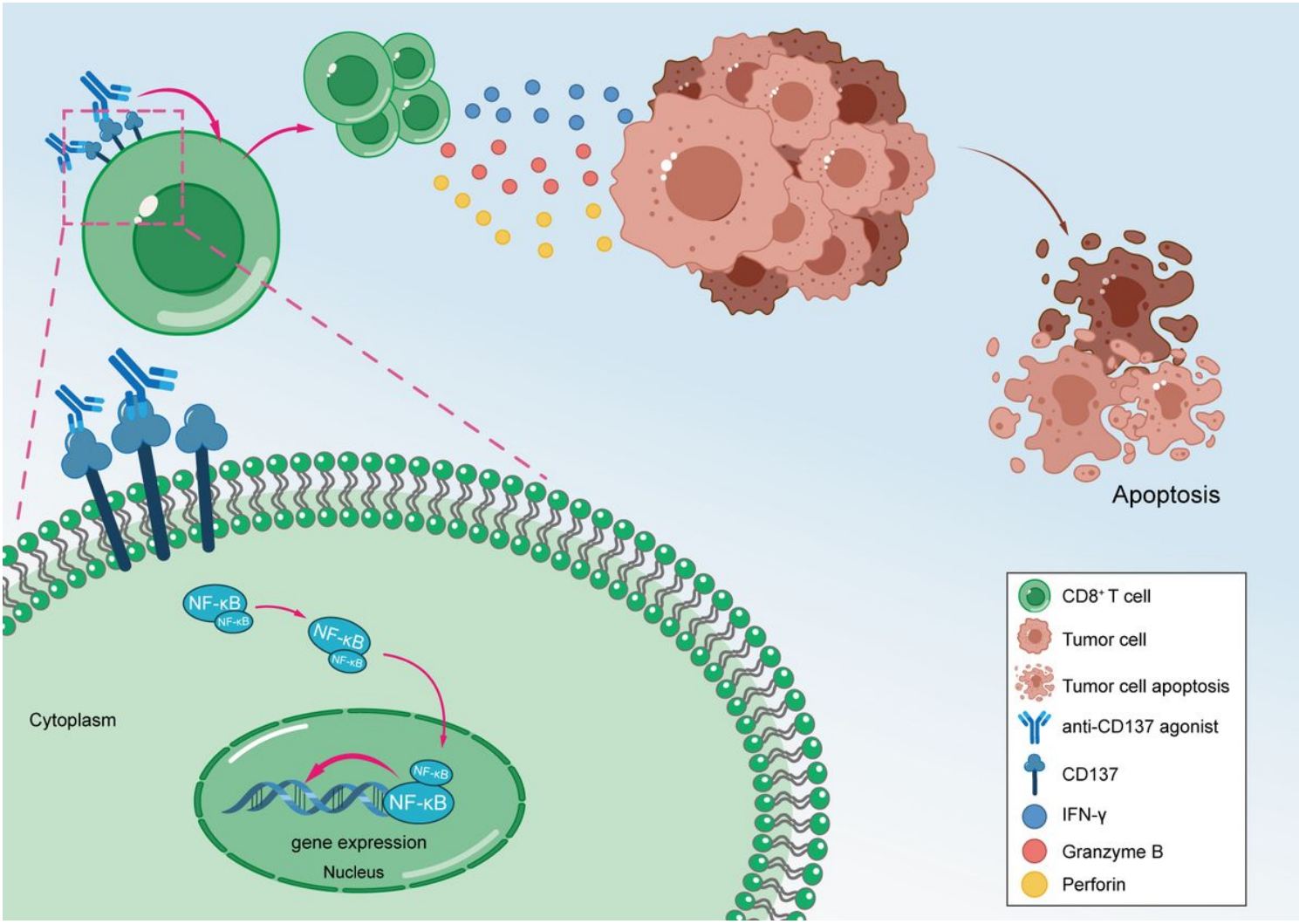

Figure 7

Schematic diagram of a CD137 agonist in inducing GC apoptosis by enhancing CD8+ T cells functions.